NOTES AND CORRESPONDENCE

NASA MODIS Previews NPOESS VIIRS Capabilities

THOMAS F. LEE AND STEVEN D. MILLER

Naval Research Laboratory, Monterey, California

CARL SCHUELER AND SHAWN MILLER

Santa Barbara Remote Sensing, Raytheon, Santa Barbara, California

(Manuscript received 5 April 2005, in final form 13 December 2005)

ABSTRACT

The Visible/Infrared Imager Radiometer Suite (VIIRS), scheduled to fly on the satellites of the National Polar-orbiting Operational Environmental Satellite System, will combine the missions of the Advanced Very High Resolution Radiometer (AVHRR), which flies on current National Oceanic and Atmospheric Administration satellites, and the Operational Linescan System aboard the Defense Meteorological Satellite Program satellites. VIIRS will offer a number of improvements to weather forecasters. First, because of a sophisticated downlink and relay system, VIIRS latencies will be 30 min or less around the globe, improving the timeliness and therefore the operational usefulness of the images. Second, with 22 channels, VIIRS will offer many more products than its predecessors. As an example, a true-color simulation is shown using data from the Earth Observing System's Moderate Resolution Imaging Spectroradiometer (MODIS), an application current geostationary imagers cannot produce because of a missing "green" wavelength channel. Third, VIIRS images will have improved quality. Through a unique pixel aggregation strategy, VIIRS pixels will not expand rapidly toward the edge of a scan like those of MODIS or AVHRR. Data will retain nearly the same resolution at the edge of the swath as at nadir. Graphs and image simulations depict the improvement in output image quality. Last, the NexSat Web site, which provides near-real-time simulations of VIIRS products, is introduced.

1. Introduction

The Visible/Infrared Imager Radiometer Suite (VIIRS), scheduled to fly on the National Polar-orbiting Operational Environmental Satellite System (NPOESS) satellites, will combine and replace the missions of the National Oceanic and Atmospheric Administration (NOAA) Advanced Very High Resolution Radiometer (AVHRR), and the Operational Linescan System (OLS) aboard the Defense Meteorological Satellite Program (DMSP) satellites. Currently images from OLS and AVHRR have a number of features that limit their use in forecasting operations compared with images from geostationary satellites. AVHRR data have relatively high spatial resolution at nadir (about 1 km), but degrade rapidly toward the edge of the swath, such that edge images are not usable for many applications. This degradation effect is minimized in OLS imagery, but the uncalibrated data are difficult to display or image process. Temporal refresh for both systems is low, and it often takes hours for data to be relayed to forecast offices. Geostationary data, on the other hand, come frequently, promptly, and cover broad regions. Operational geostationary radiometer suites, containing 5–12 channels, can now produce multispectral products once possible only from polar satellites.

NPOESS will have three specific improvements that promise to make polar images popular again among forecasters. First, the time required to deliver data from the three-satellite NPOESS network ("latency") will be greatly reduced (section 2). Second, the VIIRS sensor will provide dramatically improved images through improved scan geometry (section 3). Third, the 22 VIIRS channels will lead to new and improved forecaster

Corresponding author address: Thomas Lee, Naval Research Laboratory, 7 Grace Hopper Ave., Monterey, CA 93943.
E-mail: lee@nrlmry.navy.mil

TABLE 1. VIIRS channels in comparison with MODIS.

Band No.	VIIRS wavelength (μm)	VIIRS nadir pixel size (km): down × cross	MODIS nadir pixel size (km)	Primary application(s)
M1	0.412	0.742 × 0.259D	1.0	Ocean color, aerosols
M2	0.445	0.742 × 0.259D	1.0	Ocean color, aerosols
M3 blue	0.488	0.742 × 0.259D	0.5	Ocean color, aerosols
M4 green	0.555	0.742 × 0.259D	0.5	Ocean color, aerosols
I1 red	0.640	0.371 × 0.387	0.25	Imagery, vegetation
M5	0.672	0.742 × 0.259D	1.0	Ocean color, aerosols
M6	0.746	0.742 × 0.776	1.0	Atmospheric correction
I2	0.865	0.371 × 0.387	0.25	Vegetation
M7	0.865	0.742 × 0.259	1.0	Ocean color, aerosols
Day–night	0.7	0.742 × 0.742	N/A	Imagery
M8	1.24	0.742 × 0.776	0.5	Cloud particle size
M9	1.38	0.742 × 0.776	1.0	Cirrus cloud cover
M10	1.61	0.742 × 0.776	0.5	Binary snow map
I3	1.61	0.371 × 0.387	0.5	Snow cover
M11	2.25	0.742 × 0.776	0.5	Clouds
M12	3.70	0.742 × 0.776	1.0	SST
I4	3.74	0.371 × 0.387	1.0	Imagery, clouds
M13	4.05	0.742 × 0.259D	1.0	SST, fires
M14	8.55	0.742 × 0.776	1.0	Cloud-top properties
M15	10.76	0.742 × 0.776	1.0	SST
I5	11.45	0.371 × 0.387	1.0	Cloud imagery
M16	12.01	0.742 × 0.776	1.0	SST

products (section 4). As an example, we show a true-color simulation, based on data from the Moderate Resolution Imaging Spectroradiometer (MODIS), a research imager aboard the Earth Observing System (EOS) satellites. The paper closes with a discussion of the NexSat Web site (section 5) for viewing near-real-time simulations of future VIIRS products.

2. Improved latency

At the present, forecasters located at a facility with a direct readout station can create polar-orbiting products in real time, but only for the region viewed during line-of-sight contact with the receiver. Forecasters without such capability must typically wait 2–3 h after overpass time to receive the same information, diminishing the usefulness of polar-orbiting products in operational forecasting support. Through a sophisticated "safety net" consisting of a multiple-downlink and fiber optic data relay system, NPOESS products will be available in fewer than 30 min from overpass time, even for forecasters situated thousands of miles away from the imaged scene (Jones et al. 2004a). At the height of the NPOESS era (a triad of satellites operating simultaneously), there will be three sets of daylight overpasses per 24-h period, supplementing the more frequent geostationary data collection (Jones 2004). VIIRS will also be installed on the NPOESS Preparatory Project satellite, a predecessor satellite to NPOESS, scheduled for launch in 2009 (Jones et al. 2004b) with product latency of about 2 h.

3. VIIRS spatial resolution and improved scan geometry

The 22 VIIRS channels are situated at wavelengths similar to MODIS (Table 1). Two spatial resolutions will be employed. "Imaging" (I) channels will have a spatial resolution of about 0.38 km at nadir (0.371 km down track and 0.387 km cross track). "Moderate" (M) channels will have a spatial resolution of about 0.76 km at nadir (0.742 km down track and 0.776 km cross track). Some of the moderate channels will have dual (D) gains, capable of measurement within two discrete ranges of radiance (Table 1). The spatial resolutions of the D channels will be converted to the moderate resolution listed above (0.76 km) by ground processing. The true-color input channels on VIIRS, simulated in section 4 using MODIS data, are blue (~0.49 μm; moderate resolution), green (~0.55 μm; moderate resolution), and red (~0.64 μm; imaging resolution).

VIIRS (Scalione et al. 2004) will have a swath of about 3000 km versus about 2800 km for AVHRR and 2330 km for MODIS. However, the larger swath understates the VIIRS improvement in forecaster quality compared with MODIS. For MODIS, a much more pronounced expansion of pixels occurs in the cross-track than in the down-track direction (Fig. 1). How-

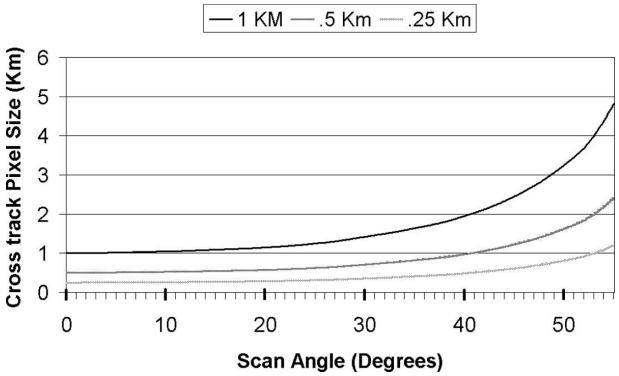

FIG. 1. MODIS cross-track variation in pixel size as a function of scan angle away from nadir. Half- and quarter-kilometer data are used in construction of true-color images.

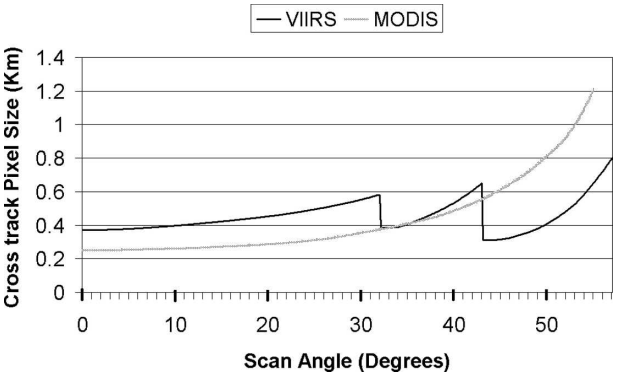

FIG. 3. Comparison of cross-track pixel size for high-resolution red input channels required for true color: VIIRS 0.38-km (nadir) resolution vs MODIS 0.25-km (nadir) resolution.

ever, through a procedure described below, cross-track pixel expansion will be limited for VIIRS (Fig. 2) and a nearly square pixel size will be maintained throughout the swath (Nishihama et al. 1997). Plotting both VIIRS and MODIS functions together (the finest resolution for each) predicts how VIIRS will produce more uniform imagery than MODIS across a scene (Fig. 3).

The VIIRS instrument will improve cross-track image quality by a unique aggregation method (Schueler 1997), inspired by a similarly motivated strategy used by DMSP OLS (Johnson et al. 1994). For each scan the VIIRS imager will employ a set of "subdetectors" to produce a sequence of "subpixels," each smaller than the nominal pixel size in Fig. 2. The subpixels within this sequence will grow toward the edge of the swath in a similar fashion to MODIS. To produce the functions in Fig. 2, however, the data from adjacent subdetectors will be combined in onboard processing to yield a series of macropixels at nominal resolution. From about 0° to 32°, three subpixels will be combined to make one nominal pixel. From about 32° to 43°, two subpixels will be combined to make a nominal pixel. Finally, from about 43° to the edge, the subpixels will not be combined, such that the subpixel and the nominal pixel size will be the same. This strategy, which explains the discrete switches observed in Fig. 2, will produce a higher signal to noise ratio (SNR) near nadir where more aggregation occurs; SNR will be lower at the edge of swath where there is no aggregation. However, SNR at the edge will still exceed a priori VIIRS instrument requirements and will be comparable to that of MODIS.

For most other channels, especially in the middle and far infrared, the overall improvement of the spatial resolution of VIIRS compared with MODIS (Table 1) is significantly greater than in Fig. 3, both at nadir and the edge of swath (representative comparison shown in Fig. 4). This improvement follows because all 22 VIIRS channels will be at 0.76 km or better at nadir. In con-

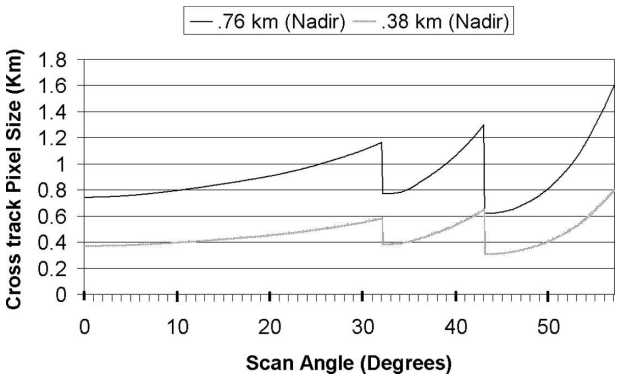

FIG. 2. VIIRS cross-track variation in pixel size as a function of scan angle away from nadir. Both resolutions will be used in the construction of true color.

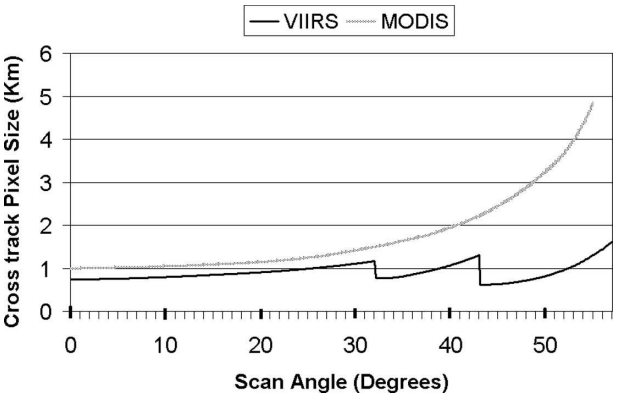

FIG. 4. Comparison of 1-km (nadir) resolution used for 29 of 36 MODIS channels with 0.76-km (nadir) resolution for VIIRS at moderate resolution. Of the 22 VIIRS channels, 17 use the resolution shown here. Five use a higher resolution of 0.38 km (nadir).

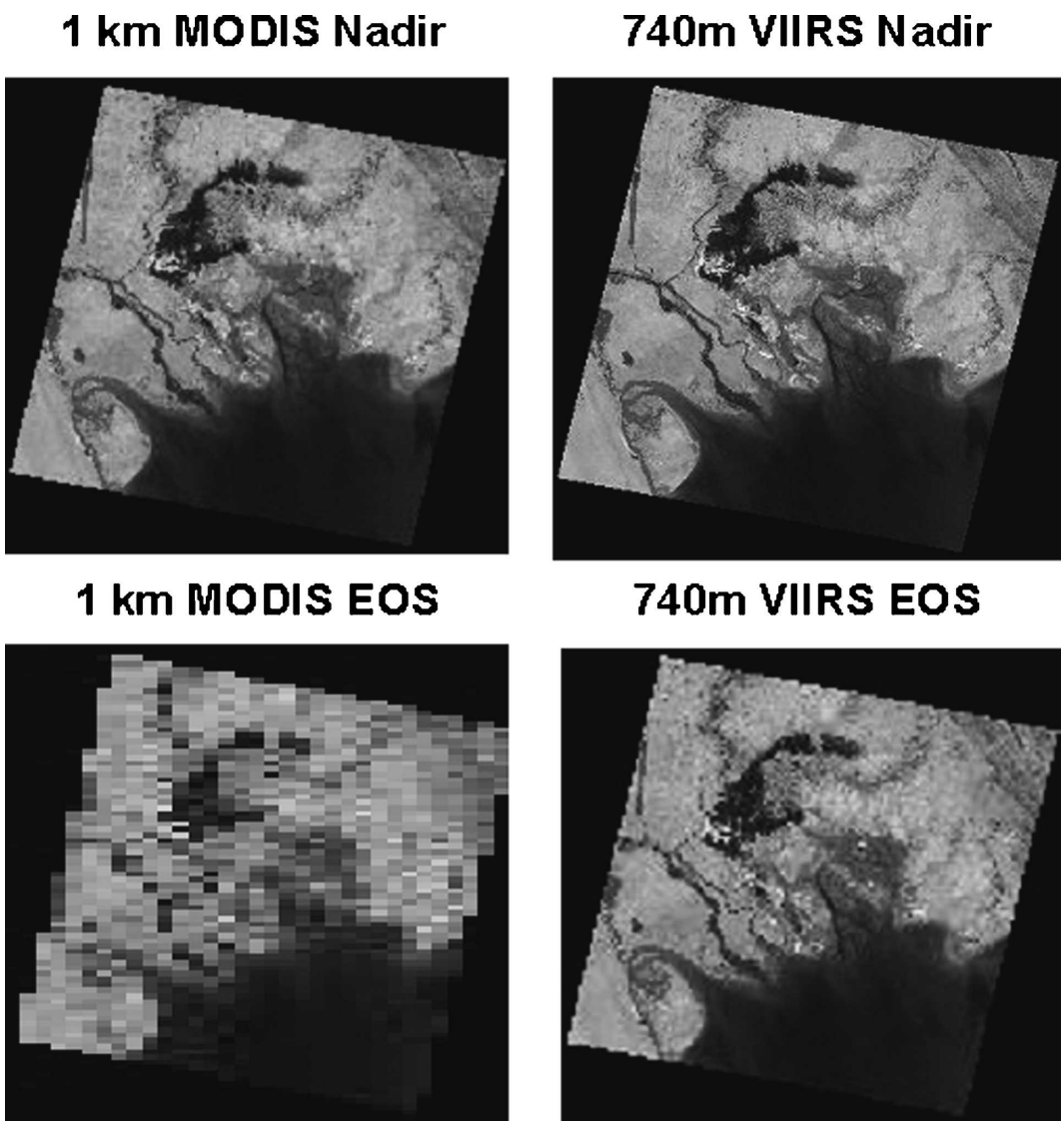

FIG. 5. Simulation comparing simulated MODIS and VIIRS images at (top) nadir and (bottom) the edge of swath (EOS). The extreme northern Persian Gulf, including portions of Kuwait and southern Iraq, is shown.

trast, 29 out of 36 MODIS channels are at 1 km at nadir, comparable to AVHRR. As before, pixel expansion is reduced with VIIRS.

Higher-resolution Landsat Thematic Mapper (TM) visible data are used to simulate the improvement of VIIRS with respect to MODIS over the northern Persian Gulf (Fig. 5), comparing the 1-km (nadir) MODIS resolution to the 0.76-m (nadir) VIIRS resolution. We do this by selectively aggregating the TM data to take the different scan geometries into account. For example, a 1 km $\times$ 1 km nadir MODIS pixel is simulated by averaging the radiances for a 33 $\times$ 33 block of Landsat 30-m pixels; a 2 km $\times$ 6 km MODIS pixel at the edge of the swath is simulated by averaging the radiances for a 67 $\times$ 200 block of Landsat 30-m pixels. Near nadir the level of detail in the simulations is similar; however, the appearance of the MODIS degrades significantly toward the edge. The appearance of the VIIRS image, though minimally degraded, is distinctly sharper.

This improvement in VIIRS will have a positive impact on forecasters. With MODIS, unsuspecting users can get confused when one image is sharp and well defined (at nadir), and the next image of the same region (at the edge of swath) is degraded. Many do not know about scan geometry effects and can therefore be baffled. With VIIRS, users will get consistent images regardless of the position of the region of interest within the swath.

4. VIIRS true-color demonstration

Though long familiar to remote sensing professionals, true-color imaging is new to most forecasters since operational weather satellites do not contain the requisite channels. It is one of the most conspicuous imaging advances anticipated with VIIRS, and we demonstrate it here using MODIS data. Figure 6 shows San Francisco, California, based on the MODIS sensor aboard the *Terra* (1030 equator crossing time) satellite; similar MODIS images are available from the *Aqua* (1330 equator crossing time) satellite. Each satellite gives about two regional coverage images per 24-h period over the midlatitudes, more toward the poles and fewer toward the Tropics. We compare it with a Geostationary Operational Environmental Satellite (GOES) image (Fig. 6, top) at about the same time.

The true-color rendition (Fig. 6, bottom) reveals coastal stratus impinging upon the green forests of the Santa Cruz Mountains; gray urban detail appears in the Santa Clara ("Silicon") Valley in the lee of these mountains (locations in Fig. 7). Farther inland, a range of hills known as the East Bay Hills is depicted in shades of brown. In the San Pablo Bay brown turbid waters contrast with bluer waters in the extreme southern end of San Francisco Bay. Stratus clouds can be seen pouring into San Francisco Bay through the gap spanned by the Golden Gate Bridge. Most of the cloud features appear in the GOES image taken at the same time, but they lack the sharpness and clarity inherent in the 250-m resolution MODIS true-color example. Offshore, the white regions correspond to optically thick clouds in the true-color image, and varying shades of blue reveal the ocean beneath broken cloud cover.

True-color images offer a number of qualitative advantages over their panchromatic or false-color counterparts. First, true color is attractive because it simulates what is familiar to the human eye: water appears dark blue, vegetation appears green, desert appears in shades of brown, cities often appear gray, and cloud and snow cover appear white. The images are not just colorful but allow the observation of fine spatial detail, blending information from the MODIS blue channel (500-m resolution), green channel (500-m resolution), and red channel (250-m resolution). The green and blue channels, which exist at the 500-m native resolution, have been synthesized to 250-m resolution by assigning an intrapixel variance specified by the 250-m native resolution red channel. The underlying assumption is that subgrid-scale variability is similar among the three channels. The technique is enabled by the carefully designed nesting between the 250-, 500-, and 1000-m grids that allows for representation of the coarser grids through linear combination of the finer grid pixels.

While true color can be approximated from other satellite data streams lacking these channels, invariably these simulations result in a loss of information or introduction of spurious artifacts. Geostationary images hold an inherent advantage over polar-orbiting images because of their high temporal refresh. However, even the radiometer planned for the next-generation *GOES-R* series lacks true-color capability (no green channel as in Table 1).

The application of true-color images to operational environmental monitoring was foreseen by Gumley and King (1995) who used MODIS Airborne Simulator data to observe floods. In the atmospheric research literature, the imaging of aerosols is probably the most significant application of true-color images to date. Dust, smoke, and air pollution tend to disappear in monochromatic satellite images but often appear dramatically in true color and are used to provide context to other scientific results (Chu et al. 2003; Ichoku et al. 2003; King et al. 2003; Koren et al. 2004; Li et al. 2003). General VIIRS scientific algorithms for clouds are foreseen by Pavolonis and Heidinger (2004) and Pavolonis et al. (2005).

5. NexSat Web site

The Naval Research Laboratory hosts near-real-time true-color examples from MODIS similar to the example here on its NexSat Web site (http://www.nrlmry.navy.mil/NEXSAT.html). Developed under the auspices of the NPOESS Integrated Program Office (http://www.ipo.noaa.gov/), NexSat displays products from operational and research satellites to anticipate the improvements coming with the next-generation VIIRS system aboard NPOESS. In addition to true-color close-ups of over 50 major cities across the continental United States, NexSat features a variety of other products covering regional and national (lower 48 states) scales, including cloud-top heights, cloud properties, blowing dust (Miller 2003), cloud layers, cirrus, cloud over snow cover, contrails, vegetation index, low clouds at night, and nighttime light detection. EOS MODIS, NOAA AVHRR, DMSP OLS, and *GOES East*/*West* imagers all supply NexSat with a comprehensive array of near-real-time products. With online training modules for each product and an extensive online archive, NexSat appeals to an audience that includes the academic, private sector, government, and general public communities.

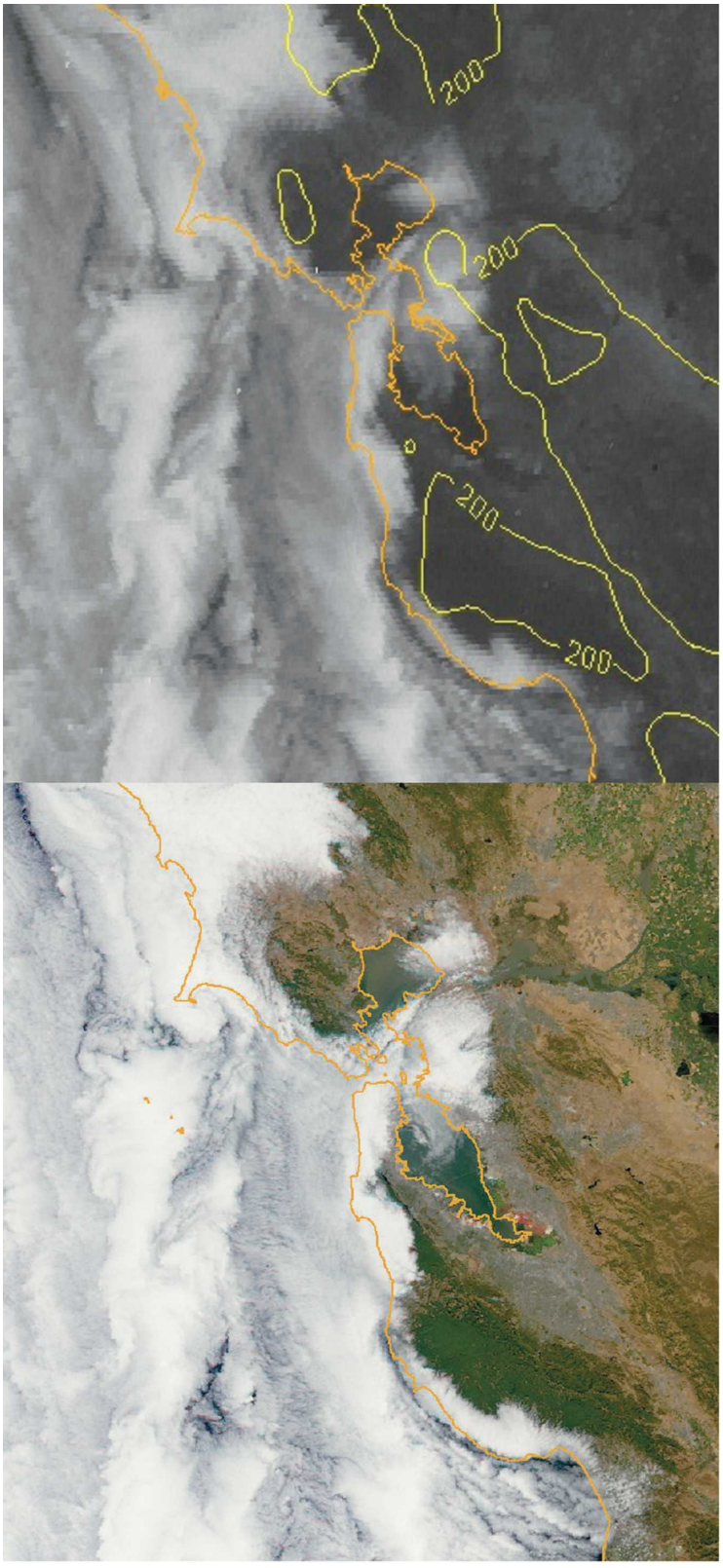

FIG. 6. (top) *GOES-West* visible image at 1845 UTC 29 Jul 2004. The yellow contour represents the 200-m terrain elevation level. (bottom) *Terra* MODIS true-color image at 1855 UTC 29 Jul 2004. The image is of central CA; stratus covers the offshore waters to the west and extends inland into the San Francisco Bay region. The coastlines are drawn in orange.

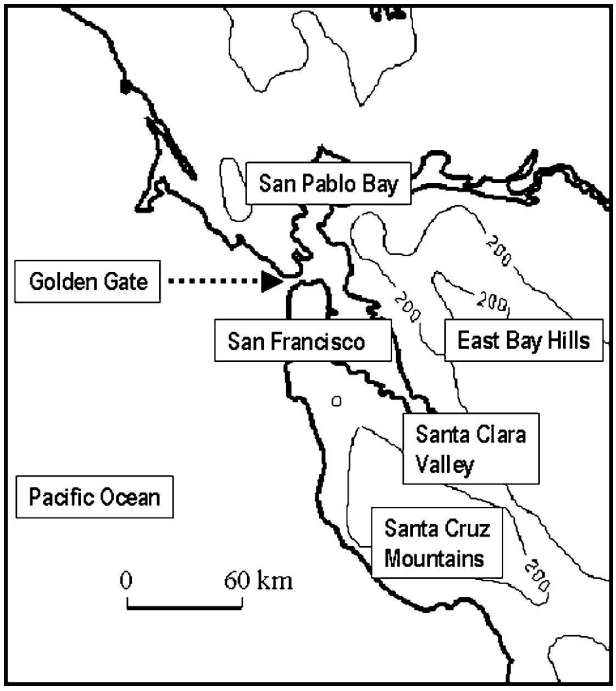

FIG. 7. The study area for Fig. 6.

6. Conclusions

VIIRS will supply a large number of products to complement the more frequent forecast support from geostationary imagers, including true color. (Geostationary imagers do not—and most will not in the foreseeable future—create true-color images because of a missing green wavelength channel.) Quality and timeliness will increase for many VIIRS additional products. All 22 VIIRS channels will have 0.76 m or better spatial resolution at nadir. In contrast for MODIS, 29 out of 36 channels are at 1 km at nadir, comparable to AVHRR. Furthermore, VIIRS will have a wider swath width and suffer less image quality degradation toward the edge of swath than either predecessor instrument.

Acknowledgments. The MODIS data used in this study were acquired as part of NASA's Earth Science Enterprise through the NASA Goddard Distributed Active Archive Center. The support of the research sponsor, the NPOESS Integrated Program Office, located in Silver Spring, Maryland, is gratefully acknowledged.

REFERENCES

Chu, D. A., Y. J. Kaufman, G. Zibordi, J. D. Chern, J. Mao, C. Li, and B. N. Holben, 2003: Global monitoring of air pollution over land from the Earth Observing System-Terra Moderate Resolution Imaging Spectroradiometer (MODIS). *J. Geophys. Res.,* **108,** 4661, doi:10.1029/2002JD003179.

Gumley, L. E., and M. D. King, 1995: Remote sensing of flooding in the U.S. upper midwest during the summer of 1993. *Bull. Amer. Meteor. Soc.,* **76,** 933–943.

Ichoku, C., L. A. Remer, Y. J. Kaufman, R. Levy, D. A. Chu, D. Tanre, and B. N. Holben, 2003: MODIS observation of aerosols and estimation of aerosol radiative forcing over southern Africa during SAFARI 2000. *J. Geophys. Res.,* **108,** 8499, doi:10.1029/2002JD002366.

Johnson, D. B., P. Flament, and R. L. Bernstein, 1994: High resolution satellite imagery for mesoscale meteorological studies. *Bull. Amer. Meteor. Soc.,* **75,** 5–33.

Jones, D., 2004: The future of Earth—Sensing from space, the next generation satellite series: A look at NPOESS and its benefits. *Earth Obs. Mag.,* **13** (1), 4–10.

——, C. Nelson, and M. Bonadonna, 2004a: NPOESS: 21st century space-based military support. *Earth Obs. Mag.,* **13** (4), 24–30.

——, S. R. Schneider, P. Wilczynski, and C. Nelson, 2004b: NPOESS Preparatory Project: The bridge between research and operations. *Earth Obs. Mag.,* **13** (3), 12–17, 20–22.

King, M. D., S. Platnick, C. C. Moeller, H. E. Revercomb, and D. A. Chu, 2003: Remote sensing of smoke, land, and clouds from the NASA ER-2 during SAFARI 2000. *J. Geophys. Res.,* **108,** 8502, doi:10.1029/2002JD003207.

Koren, I., Y. J. Kaufman, L. A. Remer, and J. V. Martins, 2004: Measurement of the effect of Amazon smoke on inhibition of cloud formation. *Science,* **303,** 1342–1345.

Li, L., H. Fukushima, R. Frouin, B. G. Mitchell, M. X. He, I. Uno, T. Takamura, and S. Ohta, 2003: Influence of submicron absorptive aerosol on Sea-viewing Wide Field-of-view Sensor (SeaWiFS)-derived marine reflectance during Aerosol Characterization Experiment (ACE)-Asia. *J. Geophys. Res.,* **108,** 4472, doi:10.1029/2002JD002776.

Miller, S. D., 2003: A consolidated technique for enhancing desert dust storms with MODIS. *Geophys. Res. Lett.,* **30,** 2071, doi:10.1029/2003GL018279.

Nishihama, M., R. Wolfe, and D. Solomon, cited 1997: MODIS level 1A earth location: Algorithm Theoretical Basis Document version 3.0. [Available online at modis.gsfc.nasa.gov/data/atbd/atbd_mod28_v3.pdf.]

Pavolonis, M. J., and A. K. Heidinger, 2004: Daytime cloud overlap detection from AVHRR and VIIRS. *J. Appl. Meteor.,* **43,** 762–778.

——, ——, and T. Uttal, 2005: Daytime global cloud typing from AVHRR and VIIRS: Algorithm description, validation, and comparisons. *J. Appl. Meteor.,* **44,** 804–826.

Scalione, T., H. W. Swenson, F. De Luccia, C. Schueler, J. E. Clement, and L. Darnton, 2004: Post-CDR NPOESS VIIRS sensor design and performance. *Proc. SPIE Int. Soc. Opt. Eng.,* **5234,** 144–155.

Schueler, C. F., 1997: Dual-use sensor design for enhanced spatioradiometric performance. U.S. Patent 5,682,034.